Veget Hist Archaeobot (2017) 26:85–97
DOI 10.1007/s00334-015-0551-x

ORIGINAL ARTICLE

A morphometric study of variance in articulated dendritic phytolith wave lobes within selected species of Triticeae and Aveneae

Terry Ball[1] · Luc Vrydaghs[2] · Tess Mercer[1] · Madison Pearce[1] · Spencer Snyder[1] · Zsuzsa Lisztes-Szabó[3] · Ákos Pető[3]

Received: 29 June 2015 / Accepted: 11 December 2015 / Published online: 21 December 2015

Abstract Morphometric analysis has proven to be an effective tool for distinguishing among phytolith assemblages produced by closely related plant taxa. Elongate dendritic epidermal phytoliths are produced in the inflorescence bracts of many cereal species. Under light microscopy, these articulated dendritic phytoliths produce wave patterns between the margins of the cells that are reported to have taxonomic significance. In this study we explore morphometric variance among the lobes of the wave patterns formed by the articulated dendritic phytoliths within selected species of cereals as a first step towards understanding the variance between species. We found that there is often significant variance in dendritic wave lobes among different accessions of a species, among the different types of inflorescence bracts of the species (glumes, lemmas and paleae), and among each bract type's location on the inflorescence (upper, middle and lower third of inflorescence spike or panicle). We observed that shape morphometries are typically more reliable and require a smaller sample size for statistical confidence than size morphometries. We further observed that adequate samples sizes for analysis of several shape morphometries of articulated dendritic wave lobes are considerably smaller than those reported to be required for analysis of the same morphometries of individual or isolated dendritic phytoliths. To gain a preliminary sense whether there is potential for discriminating between taxa in light of the significant variance within species, we compared our data to archaeological material from the historical center of Brussels. We demonstrate that while there is considerable variance in the morphometries among accessions, bract types and inflorescence locations within each species, there may yet be potential for discriminating between cereal species in archaeological samples by the morphometries of their dendritic phytolith wave lobes. We present one possible paradigm for conducting such analysis on archaeological material.

Keywords Phytoliths · Morphometrics · Triticeae · Dendritics

Communicated by K. Neumann.

Electronic supplementary material The online version of this article (doi:10.1007/s00334-015-0551-x) contains supplementary material, which is available to authorized users.

✉ Terry Ball
terry_ball@byu.edu

[1] 210H JSB, Brigham Young University, Provo, UT 84602, USA

[2] Centre de Recherches en Archéologie et Patrimoine, Université Libre de Bruxelles, Brussels, Belgium

[3] Laboratory for Conservation and Applied Research, National Heritage Protection Centre, Hungarian National Museum, Daróci u. 3, Budapest 1113, Hungary

Introduction

Monosilicic acid, $Si(OH_4)$, in the soil is taken up by plants. Following up take the acid is transported to various plant organs, where, in many taxa, some of it polymerizes to form solid silica deposits at specific intra- and extracellular locations (Jones and Handreck 1967; Raven 1983; Sangster 1970). These solid deposits have been given the name "phytoliths", literally meaning "plant-rocks". Phytoliths often take the shape of the cell or tissue in which they form giving them potential taxonomic significance.

Phytoliths produced in plants are released into the surrounding environment when a plant's organic tissues are destroyed through processes such as decay, burning or

digestion [for a discussion on deposition see Harvey and Fuller (2005) and Madella and Lancelotti (2012)]. Such released phytoliths become microfossils of the plants that produced them. Microfossil phytoliths can be collected from a wide variety of sources including archaeological soils and palaeosols where plants once grew naturally, were cultivated or processed (e.g. Power et al. 2014; Grund et al. 2014; Devos et al. 2013; Pető et al. 2015), from rocks and drill core sediments where plant tissue may have been deposited or encapsulated (e.g. Schultz et al. 2014; Veena et al. 2014), from the coprolites and dental calculus of organisms that have consumed plants (e.g. Phillips and Lancelotti 2014; Shahack-Gross et al. 2014; Tromp and Dudgeon 2015) and from ceramics and lithics used to process or store plant materials (e.g. Gillot 2014; Liu et al. 2014; Wallis et al. 2014).

Analysis of microfossil phytoliths has proven to be a useful and informative research tool in a wide variety of disciplines including archaeology, botany, paleoecology and geology. For example, a sample of publications in early 2014 shows that Henry et al. (2014) used phytolith analysis to study the diet of Neanderthals in Europe, Africa and the Near East. Qiu et al. (2014) used phytolith analysis to document rice cultivation in the mid-Holocene in east China. Umemura and Takenaka (2014) used phytolith analysis to study the silica cycle in bamboo forests in central Japan and Cotton et al. (2014) used phytolith analysis to reconstruct paleoclimates and suggest tectonic control on the expansion of C-4 grasses during the late Miocene and early Pliocene in northwest Argentina. While this is only a small sample of the many studies employing phytolith analysis published during the year 2014, it serves to illustrate the depth and breadth of the use of the research tool across many disciplines.

When conducting phytolith analysis the ability to identify the taxa that produce a microfossil assemblage of phytoliths is a critical and challenging task. While some taxa produce very distinctive phytoliths at broad taxonomic levels, for example the widely cited and utilized Twiss et al. (1969) panicoid, chloridoid and pooideae classifications for grass short cell phytoliths, closely related taxa, especially at the species level, typically produce phytoliths of similar shapes and types making their assemblages difficult to distinguish from each other. In such cases morphometric analysis (measurements of shape and/or size) of similar phytolith types has proven to provide some taxonomic resolution between closely related species (e.g. Pearsall et al. 1995; Zhao et al. 1998; Ball et al. 1999, 2006; Berlin et al. 2003; Portillo et al. 2006; Vrydaghs et al. 2009; Zhang et al. 2011; Pető et al. 2013).

Because the morphometries of phytoliths from closely related taxa usually overlap in range, it typically is not possible to distinguish between the taxa using individual phytoliths or even small sample sizes. Rather, the differences between the morphometries of phytoliths produced by closely related taxa usually are only apparent in the means of the measurements taken from large sample sizes (Ball et al. 1999). Unfortunately, adequately large sample sizes of microfossil phytoliths that researchers are confident derive from a single taxa are not commonly found. Articulated phytoliths, often called silica skeletons, provide an exception. While individual phytoliths are often found in microfossil assemblages, so too are silica skeletons or groups of phytoliths still articulated or joined together in situ assuring researchers that each derives from the same taxon and plant. Several factors may influence the amount and size of articulated phytoliths observed in a sample such as the amount of water available to the plant that produced the sample (Madella et al. 2009; Rosen 1992b), taphonomy (Madella and Lancelotti 2012; Shillito 2011a) and laboratory extraction methodology (Cabanes et al. 2011; Jenkins 2009; Shillito 2011b). We note that the archaeological record of articulated phytoliths is not restricted to silica skeletons. Articulated phytoliths have also been observed in thin sections of archaeological deposits. In soil thin sections, in addition to silica skeletons, articulated phytoliths can be either contiguous, synonymous for Shillito's (2011a) "conjoined cells", or fan shaped (for a discussion of different forms of articulated phytoliths see Albert et al. 2008; Devos et al. 2013; Shillito 2011b; Vrydaghs 2014). As the making of the soil thin sections keeps disturbance of the soil components to a minimum, the technique avoids all laboratory extraction factors that may influence the amount and size of articulated dendritics. Articulated phytoliths can often provide a large enough sample for statistical confidence in analysis of some morphometric variables (Vrydaghs et al. 2015).

Articulated dendritic phytoliths

Elongate dendritic epidermal phytoliths, hereafter referred to simply as dendritics, are produced in the epidermal long cells of the inflorescence bracts of many cereal taxa such as Triticeae and Aveneae species (Ball et al. 1999). Dendritics appear to be formed by the silicification of the lumen of inflorescence bract epidermal long cells. Like other phytolith morphotypes produced in cell lumens, such as grass epidermal short cell phytoliths, dendritics are relatively thick and robust when compared to those produced by silicification of cell walls. The dendritic processes that extend out from the lateral edges of these phytoliths may vary from being heavily branched, hence the name dendritic, to simply echinate, apparently depending on the shape of the cell lumens prior to silicification. Lumina with many intricate voids and plasmodesmata result in the formation of heavily branched dendritic processes on the

phytoliths upon silicification of the voids, while lumens with few intricate voids appear to produce more echinate processes on the phytoliths. Often both heavily branched and echinate processes may be observed on a single dendritic phytolith (Ball et al. 1999; Fig. 1a, b). Dendritics are frequently found articulated in reference and microfossil assemblages of phytoliths. Under light microscopy, articulated dendritics form wave patterns between the margins of adjacent cells that are reported to have taxonomic significance (Rosen 1992a; Fig. 1c, d).

Rosen (1992a) presents images and line drawings illustrating general differences she observed in the wave patterns of articulated epidermal phytoliths in wheat (*Triticum* sp.), barley (*Hordeum* sp.), goat grass (*Aegilops* sp.), oat grass (*Avena* sp.) and rye grass (*Lolium* sp.) husks. In her observations she notes both "thick" and "thin" wave patterns in the taxa. As we study her micrographs it appears that the "thick" waves she observes are formed between adjacent articulated dendritic phytoliths, which again are formed by silicification of epidermal cell lumens. The thickness of the waves appears to be due to the relatively wide distance between adjacent dendritic phytoliths in the silica skeletons (see Figs. 7.7, 7.8A and 7.12 in Rosen 1992a). In contrast the thin waves she notes appear to be formed not between dendritics, but rather between adjacent articulated elongate undulate epidermal phytoliths which are produced by the silicification of epidermal cell walls and are comparatively fragile and thin. The thinness of the waves appears to be due to the relatively narrow distance between adjacent undulate epidermal phytoliths in the silica skeletons (see Figs. 7.6, 7.8B and 7.12 in Rosen 1992a; see also Fig. 1c, g herein). Thus Rosen appears to view the waves as the space between the margins of adjacent cells. In our study we will follow Helbaek (1960) by viewing the waves as the contour of a single cell margin as illustrated in Fig. 1h, i. While Rosen (1992a, b) notes that her work represents a preliminary stage of investigation, we found it promising, provocative and deserving of further exploration. Though the wave patterns produced by elongate undulate epidermal phytoliths also deserve further investigation, we focus this study only on articulated dendritic waves as they are the more robust and frequently observed in microfossil assemblages. In this study, we build on Rosen's (1992a) work by analyzing additional cereal taxa and accessions of each taxon and quantifying our findings through morphometric analysis of the articulated dendritic wave lobes (Fig. 1j).

Research questions

Before analyzing the morphometric differences in dendritic waves between species, we felt it necessary to first understand the variance in the waves within each species. As observed by Out and Madella (2015), studies on variation in phytolith morphometries between taxa are abundant, but studies of variation within species are rare. Tubb et al. (1993) noted some morphometric variation in papillae within some Triticeae species. Ball et al. (1999) report the range of morphometries for various morphotypes produced in the inflorescences of several selected species of Triticeae, as do Portillo et al. (2006) for two species of Aveneae, but none of these studies directly consider the question of morphometric variation within a given species. For an example and review of the limited studies reporting phytolith morphometric variation within taxa other than Triticeae and Aveneae species see Out and Madella (2015). In this study we address four research questions in regards to within-species phytolith morphometric variation in several important species of Triticeae and one from Aveneae. First, are there significant differences in the morphometries of dendritic wave lobes produced in the different inflorescence bracts of a species, i.e. the glumes, lemmas and paleae? Second, are there significant morphometric differences in dendritic wave lobes produced by bracts on different locations on the inflorescence, i.e. upper, middle and lower thirds of the spikes or panicles? Third, are there significant differences in the morphometries of dendritic wave lobes produced in the different accessions of each species? Fourth, how many dendritic wave lobes in a given silica skeleton must be measured to have statistical confidence that the measurements accurately represent the species? Answering these questions about variance within each species is a critical first step for researchers hoping to develop reliable sampling strategies and references collections of data for distinguishing between species in future studies. To gain a preliminary sense whether there is also some potential for discriminating between taxa based on the morphometries of articulated dendritic wave lobes, we further compare our data to archaeological material from the historical center of Brussels and present one possible paradigm for identifying taxa using the morphometric data.

Materials and methods

Evaluation of variance between bracts

For the study of variance between different inflorescence bracts of a species we chose to analyze three accessions for each of four species of wheat (*Triticum aestivum, T. durum, T. dicoccoides,* and *T dicoccon* which is also known as *T. turgidum* ssp. *dicoccum*), and one species each of oats (*Avena sativa*), barley (*Hordeum vulgare*) and rye (*Secale cereale*; see Table 1). All the plants were grown at the Brigham Young University, Provo, Utah, USA greenhouse

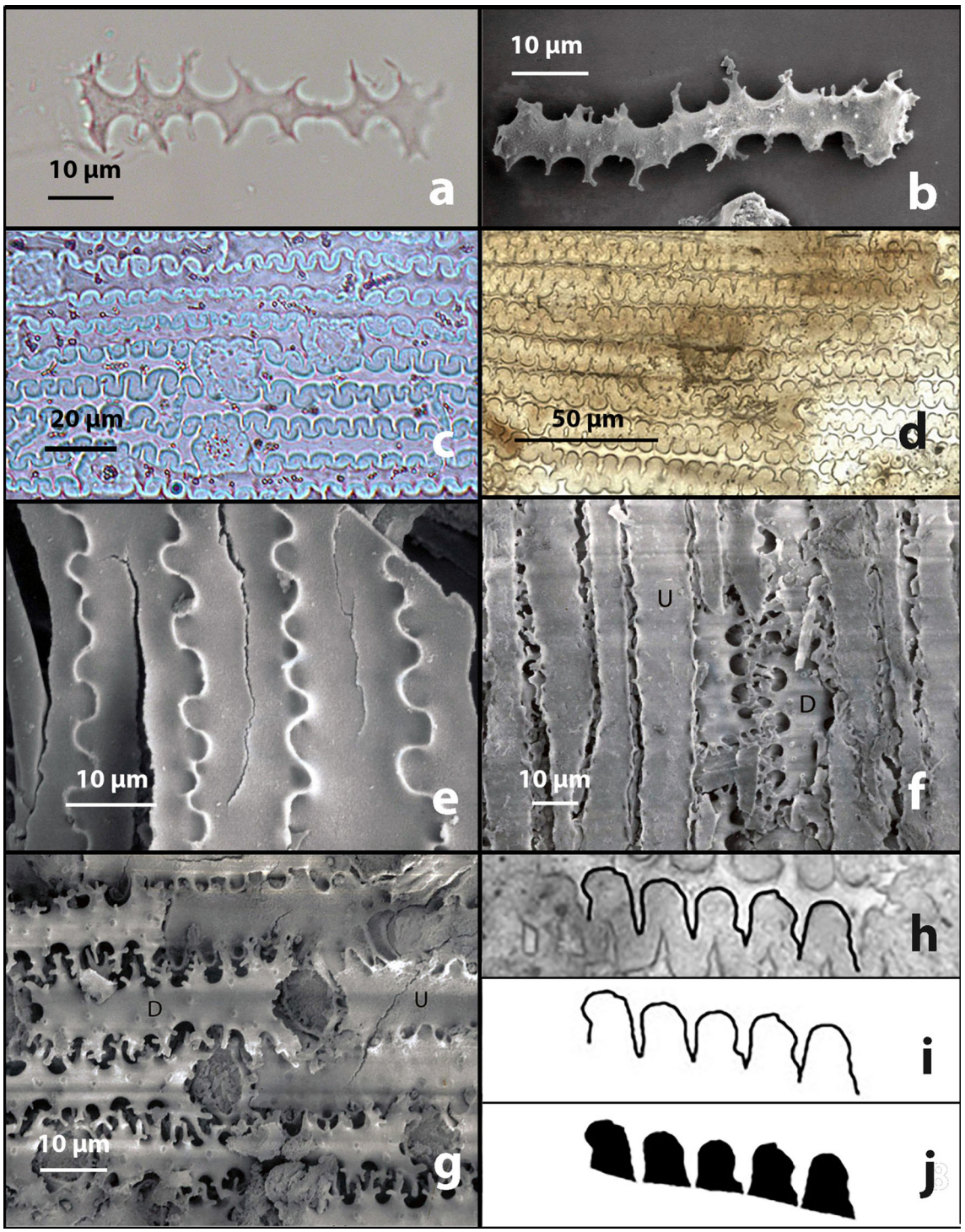

from seeds obtained from National Small Grains Collection of the USDA-ARS in Aberdeen. The plants were all grown during the same year under uniform growing conditions and harvested when mature and dry. Samples for analysis were collected from three plants for each accession, prepared for microscopy, imaged and analyzed as follows:

1. Florets taken from the middle third of inflorescence from each accession of each species were dissected and six to eight glumes, lemmas and paleae were placed in separate four-inch petri dishes. In sampling the florets we were not able to distinguish between those produced by different individual plants of the same

◀**Fig. 1** **a** Light micrograph of disarticulated elongate dendritic epidermal phytolith from *Triticum monococcum*; **b** SEM micrograph of disarticulated elongate dendritic epidermal phytolith from *Triticum monococcum* formed by silicification of epidermal cell lumen. Note thick, robust structure of the phytolith compared to Fig. 1e; **c** Micrograph of articulated elongate dendritic epidermal phytoliths produced in glumes taken from the lower portion of the inflorescence spike of *Triticum monococcum*; **d** Micrograph of archaeological microfossil articulated elongate dendritic epidermal phytoliths extracted from horse coprolites; **e** SEM micrograph of articulated elongate undulate epidermal phytoliths from *Triticum monococcum* formed by silicification of epidermal cell walls. Note the thin delicate structure of the phytoliths and the narrow margin between adjacent cells that form thin wave patterns compared to Fig. 1g; **f** SEM micrograph of articulated elongate undulate epidermal phytoliths (U) with articulated elongate dendritic epidermal phytoliths (D) exposed underneath from *Triticum aestivum.* Note undulate phytoliths form from cell wall silicification and are relatively thin, while the dendritic phytoliths underneath form from cell lumen silicification and are comparatively thick; **g** SEM micrograph of articulated elongate dendritic epidermal phytoliths (D) with exposed articulated elongate undulate epidermal phytoliths (U) underneath from *Triticum aestivum*; **h–j** Illustration of how wave patterns are processed into individual lobes for measurements

Table 1 List of species and accessions

Genus	Species	Accession #	Ref #
Triticum	*aestivum*	CI tr 6301	41
		CI tr 8240	44
		CI tr 12459	46
	durum	CI tr 1337	38
		CI tr 3119	39
		CI tr 17291	52
	dicoccon	CI tr 7962	75
		CI tr 14824	77
		PI 254156	86
	dicoccoides	PI 256029	60
		PI 300990	65
		PI 352326	68
	monococcum	400	1
Avena	*sativa*	CI av 1599	5
		CI av 2562	7
		CI av 9208	10
Hordeum	*vulgare*	CI ho 254	6
		CI ho 3856	17
		CI ho 6020	18
Secale	*cereale*	CI sc 123	34
		PI 168130	35
		PI 263750	37

All plants grown in a greenhouse from seeds obtained from National Small Grains Collection of the USDA-ARS in Aberdeen, Idaho with the exception of the *T. monococcum* samples which were collected from the experimental plots of the Research Centre for Agrobiodiversity Tápiószele, Hungary; http://www.nodik.hu/english/?page_id=42. *H. vulgare* Ref. # 6 is a six-rowed naked variety. *H. vulgare* Ref #s 17 and 18 are six-rowed hulled varieties

accession, as the inflorescence spikes from each accession had previously been harvested, mixed and stored together. We recognize that there may be some variance between individual plants of the same accession of a species, especially if they are grown in different environmental conditions, but since all these plants were grown under the same conditions we assumed that such variance would be negligible [see Ball and Brotherson (1992) for more on the effect of varying environmental conditions on phytolith morphometries].

2. 40 ml of a 50/50 mixture of household bleach and deionized water (DH_2O) were added to each petri dish to digest the inflorescence bracts until they were clear and translucent, but still articulated.
3. The bleach solution was then gently decanted and the bracts gently washed by adding DH_2O to the dishes until the bracts floated.
4. A microscope slide was placed in each of the petri dishes under the floating bracts, and then carefully lifted out to float the articulated bracts onto the slide with as little disturbance to the tissue as possible.
5. The slides were then placed in a drying oven. Once dry, coverslips were mounted over the bracts using Permount.
6. Slides thus prepared were viewed under light microscopy at ×400 magnification and ten images of randomly selected articulated dendritics from randomly selected bracts of each type for each accession of each species were collected using a digital camera attached to the microscope. We did not distinguish between dendritics formed between the edges, centres and tips of the bracts in our sampling for this study. Doing so may identify another source of variance in the morphometrics.
7. The images of dendritic waves were processed and analyzed using ImageJ software from NIH (available at http://imagej.nih.gov/ij/download.html) with a plugin and macro program we developed entitled PhytolithsBatch (Ball et al. 2015). We used this image analysis software to make the 17 standard measurements of shape and size (for a discussion and illustrations of these morphometries see Ball et al. 2015). Measurements were made by four different members of our research group. An initial comparison of the measurements made on the same sample by three different researchers found that though there were slight differences in the values obtained, the differences were not statistically significant. This observation allowed us some confidence that individual researchers would not be likely to introduce significant variance into the data obtained. To make the measurements, two five-lobe lengths of dendritic waves, for a total of ten individual lobes, were outlined on each of the ten images

collected. Individual lobes were then separated as illustrated in Fig. 1h, j. Measurements of each individual wave lobe were then made. In this way 100 individual lobes (10 lobes for each of the ten images) were measured for each bract type from each accession of each species. Typically the 100 wave lobes measured for each sample were formed by 20–40 individual dendritics articulated together, thus the morphometrics can also be thought of as deriving from a sample of 20–40 dendritics.

8. Descriptive statistics were calculated for the morphometries of the lobes and Tukey HSD tests were performed to identify morphometries with significantly different ($\alpha = 0.05$) means between the bract types within each species. We used Tukey's HSD test for this analysis because it is relatively conservative in regards to both type I (false positive) and type II (false negative) statistical errors and it allows for a single-step and simultaneous multiple pairwise comparisons of means. Tukey HSD tests using $\alpha = 0.05$ as a significance threshold will indicate significant difference for any comparisons wherein $p \leq 0.05$. We used the SAS System for Windows data analysis software (SAS Institute, Cary, North Carolina) for all statistical calculations.

Evaluation of variance between inflorescence spike locations

For the study of variance between bracts from different locations on the inflorescence spikes we analyzed one accession of each of the species studied above. We were also able to add one accession of *Triticum monococcum* which was collected from the experimental plots of the Research Centre for Agrobiodiversity Tápiószele, Hungary (http://www.nodik.hu/english/?page_id=42) for this part of the study. We hope to add additional accessions of this taxon to the reference data in the future (for more on the importance of *T. monococcum* see Ball et al. 1993). Inflorescence bracts from each species were dissected from florets taken from the upper, middle and lower thirds of the inflorescence spikes of each taxa. The extremes of the spikes, i.e. very tops and very bottoms were not excluded from the sampling. All the samples were then processed following steps 2–9 above with the exception of the *T. monococcum* samples which were processed using a dry-ashing procedure as follows:

1. The bracts were washed in a clean soap solution and placed in a sonication bath for 30 min.
2. The bracts were then placed in a muffle furnace for dry-oxidation at 500 °C for 36 h.
3. The samples were further digested in a 1:1 solution of 10 ml 3 N HCl and HNO_3 and the acid solution subsequently removed by repeatedly centrifuging (5 min; 3,000 RPM), decanting and washing in DH_2O.
4. Samples were next dried in a muffle furnace and then treated with a 10 ml 30 % H_2O_2 solution and dried again.
5. The dried plant material (ash) for each sample was transferred to a microscope slide. After adding glycerin the sample was covered with a cover slip.
6. Images of articulated dendritic phytoliths in each sample were collected at a magnification of ×400 with a Leica DM2500 light microscope using a Leica DFC450 digital microscope camera equipped with a 5 megapixel CCD camera and processed using Leica Application Suite (LAS) 4.4.
7. Morphometric analysis of the articulated dendritic phytoliths in the images was then conducted as outlined in steps 7–8 above.

Evaluation of variance between accessions of each species

Tukey HSD tests were again performed to identify wave lobe morphometries with significantly different means between the different accessions of each species. To avoid any variance due to bract type or bract location on the inflorescence, we only compared glumes to glumes, lemmas to lemmas and paleae to paleae, and only evaluated the means of samples taken from the middle third of the inflorescences, thus we used the same means as those evaluated in our first study of variance between bract types, but made these different comparisons in the Tukey tests.

Evaluation of minimum adequate sample sizes

To determine minimum adequate sample sizes to ensure a 90 % confidence level that the sample means obtained were within 5 % of the actual population means, we used the standard equation: $N_{min} = Z^2_{\alpha/2} \times S^2/(ME)^2$ where N_{min} = the minimum adequate sample size, $Z^2_{\alpha/2} = 1.64$, which is the square of the two-tailed Z value at $\alpha = 0.10$, S^2 = the variance and $(ME)^2$ = the square of the desired margin of error, in this case 0.05 times the sample mean.

Results

Despite the hope of finding little or no significant variation in the wave morphometries of the different accessions, bract types and inflorescence locations within each species we analyzed, which would have simplified the sampling

and gathering of reference data for a future study of the variance between taxa, we instead found significant variance within each species. The raw data measurements and descriptive statistics for each of our samples are found in ESM 1 and 2 respectively.

Bract type variance

The results of our study of variance between bract types within an accession are reported in ESM 3 Table 1 for size morphometries and ESM 3 Table 2 for shape morphometries. These tables present the mean morphometries of 100 wave lobes measured from each bract type from each accession from each species and the results of the Tukey HSD tests for significant differences between the means of the bract types within each accession. Mean values shaded in grey in the tables are significantly different ($\alpha = 0.05$) from the others according to the Tukey HSD tests. For example, in the entry in ESM 3 Table 1 for *T. aestivum* reference accession 41, we observe that for the first morphometry of Area the mean of 100 wave lobes from the paleae is 30.0 μ^2 and that it is significantly different (shaded grey), than the mean Area of the 100 lobes we measured in the glumes (mean of 35.0 μ^2) and the lemmas (mean of 35.8 μ^2). However, the means of the lemmas and glumes are not significantly different from each other and therefore not shaded grey. Similarly, we observe in ESM 3 Table 1 that in *T. durum,* the means for all the size morphometries (i.e. Area, Convex Area, Perimeter etc.) of the glumes of reference accession 38 are significantly larger (again shaded grey) than the means of the lemmas and paleae in the accession, while in reference accession 39 all the glume means are significantly smaller than the lemmas and paleae. In contrast, in *Secale cereale* we observe in ESM 3 Table 1 that nearly every size mean of every bract is significantly different within each accession.

There does not appear to be a consistent or general pattern of variance in the data. Rather than further attempting to detail in this report all the significant differences observable in the ESM 1–3 we would simply note that generally speaking when analyzing the tables, the more grey shaded cells observed, the greater occurrence of significant differences between the mean morphometries of the different bract types within each accession. We observe that size morphometries of the different bract wave lobes within each accession (ESM 3 Table 1) were significantly different in approximately 63 % of the samples (355 out of 567), while shape morphometries (ESM 3 Table 2) varied significantly in only about 33 % of the samples (168 out of 504), indicating that the shape morphometries of the waves may be more reliable than size morphometries in distinguishing between taxa in future studies.

Inflorescence location variance

The results of our study of wave lobe morphometric variance within an accession due to the location of a bract type on an inflorescence are reported in ESM 3 Table 3 for size morphometries and ESM 3 Table 4 for shape morphometries. These tables present the means for each of the 17 morphometries for each bract type from each inflorescence location (i.e. upper, middle and lower third of the spikes or panicles) from one accession of each species analyzed and the results of the Tukey HSD tests for significant differences between the wave lobe morphometric means. A general review of ESM 3 Tables 3 and 4 illustrates that there are indeed significance differences in many of the morphometries of the wave lobes produced by the same bract type within an accession depending upon the location the bract formed on the inflorescence spike. While no consistent or general pattern of variance is apparent in the data we do observe that once again the size morphometries seem more variable than the shape morphometries. In this study the size morphometry means varied significantly due to bract location on the inflorescence in about 47 % of the samples (304 out of the 648) while the shape morphometry means varied in only about 30 % of the samples (171 out of 576).

Accession variance

After observing the great variance in wave lobe morphometries between bract types and bract inflorescence location within each accession, we assumed we would find equal variance in our tests for significant differences between the actual accessions. The assumption proved to be true. The results of our study of wave lobe morphometric variance between accessions are reported in ESM 3 Table 5 for size morphometries and ESM 3 Table 6 for shape morphometries. In summary we observe that the mean wave lobe size morphometries of the same bract types taken from the same inflorescence locations varied significantly between the accessions in 63 % (359 out of 567) of our samples while the mean shape morphometries varied significantly between the accessions in 35 % (179 out of 504) of our samples. Once again we observed no general or consistent pattern of variance, other than the fact that size morphometries between accessions varied more than shape morphometries.

Minimum adequate sample sizes

The results of our tests for adequate sample sizes for statistical confidence in wave lobe morphometric data are summarized in Table 2. As the equation for calculating N_{min} given above indicates, minimum adequate samples

Table 2 Results of tests for minimum adequate sample size (N_{min})

Size morphometry	N_{min}	Shape morphometry	N_{min}
Convex area	500	Elongation	120
Fiber length	450	Aspect ratio	50
Perimeter	310	Roundness	50
Area	290	Form factor	30
Length	120	Solidity	20
Inscribed radius	110	Compactness	20
Convex perimeter	100	Convexity	10
Breadth	80	Curl	10
Equivalent diameter	70		

Only the largest N_{min} among the samples analyzed is reported for each morphometry. All values rounded up to the nearest 10

sizes are dependent upon the amount of variance in a sample. Thus, samples with little morphometric variance will have a smaller N_{min} than samples with larger variance. We calculated the N_{min} for each morphometry for each of the more than 2,000 samples included in this study. In Table 2 we report only the largest N_{min} calculated for each morphometry among all the samples or treatments analyzed. By using these largest N_{min} values when gathering dendritic wave lobe morphometries researchers can have statistical confidence in the data obtained regardless of the taxa, accession, bract or bract location being studied. As Table 2 illustrates, because of the greater variance, much larger sample sizes are typically required to have statistical confidence in the data for size morphometries than that required for shape morphometries. We observed that while sample sizes of 100 or more are often required for statistical confidence in size morphometries, a sample size as small as 30 wave lobes can be adequate for a 90 % confidence level the sample means obtained are within 5 % of the actual population means for five of the shape morphometries: Form Factor, Solidity, Convexity, Compactness and Curl. We note that this minimum adequate sample size for these five shape morphometries of articulated dendritic wave patterns is considerably smaller than those reported by Portillo et al. (2006) who made the same measurements on entire isolated dendritics to discriminate between two *Avena* species (*A. sativa* and *A. strigosa*). This is because the morphometric variance in wave lobes is not as great as the variance in whole dendritics.

Discussion

Our findings clearly affirm that there are often significant differences in wave lobe morphometries between bract types and bract inflorescence location within accessions, as well as significant differences between the accessions themselves. Accordingly, when preparing reference data, researchers should sample not only many accessions of the taxa of concern, but also assure that all bract types from all inflorescence spike locations are sampled and measured separately for each accession. Further, because they vary less within a species, shape measurements should be considered more reliable than size measurements in reference data collections and also when attempting to use the morphometric data to distinguish among taxa. This is an encouraging finding as Ball and Brotherson (1992) observed that while size morphometries may be greatly influenced by varying environmental conditions shape morphometries generally are not. Thus relying primarily on shape morphometries may reduce concerns about whether or not environmental factors influence the data (for more examples of the value of shape morphometries see Ball et al. 1999; Out and Madella 2015; Portillo et al. 2006).

The variance we observed within accessions between bract types and inflorescence locations led us to further question if there might also be significant variance in wave lobe morphometries due to the location within the bracts where the dendritics formed, for example, would wave lobes formed in the middle of a given bract type vary significantly from wave lobes formed at the bottom, top, or edges of the bract. However, because none of our samples had dendritics formed throughout the entire bract, or even in any specific pattern we were unable to test for such variation in this study. Future studies with more uniformly silicified bracts may make such a study possible. Once we have analyzed this additional possible source of within species variance, and with the understanding this study of within species variance has given us, we hope to begin our study of between species variance in an informed and logical way. A first step will be to expand our reference data with more accessions of each taxon to assure robust results.

The discovery that the minimum adequate sample size for some morphometries of shape can be as few as 30 wave lobes may help to resolve two challenges typically encountered by researchers attempting to use morphometrics to identify taxa in archaeological samples. As discussed earlier, typically morphometric discrimination between closely related taxa is based on the differences between the mean measurements of large sample sizes, rather than measurements of individual phytoliths or small sample sizes. Unfortunately, finding adequately large sample sizes of individual disarticulated phytoliths that researchers are confident all derive from the same taxon in an archaeological sample is a rare occurrence. However, it is not uncommon in archaeological samples and thin sections to find articulated phytoliths with as few as 6–10 dendritics between which 30 or more measurable wave lobes are formed. When analyzing such articulated

Table 3 Selected mean shape morphometries of archaeological articulated dendritic wave lobes

Sample	1	2	3	4	5	6	7	8	9	10	11	12	13	14	15	16	17	18	19
ND	13	12	13	8	9	11	15	18	16	12	8	9	15	14	12	18	21	13	17
NL	30	35	30	30	30	40	45	80	40	40	30	30	40	35	30	30	70	30	80
Form Factor	0.705	0.761	0.684	0.685	0.731	0.770	0.689	0.755	0.679	0.755	0.705	0.682	0.734	0.756	0.734	0.767	0.751	0.758	0.684
Convexity	0.941	0.951	0.944	0.955	0.950	0.954	0.945	0.952	0.941	0.950	0.941	0.946	0.949	0.957	0.950	0.953	0.951	0.954	0.954
Solidity	0.952	0.989	0.971	0.990	0.984	0.989	0.971	0.977	0.950	0.989	0.955	0.994	0.992	0.992	0.972	0.993	0.974	0.994	0.991
Compactness	0.741	0.776	0.717	0.683	0.739	0.784	0.711	0.782	0.738	0.771	0.753	0.696	0.751	0.761	0.765	0.796	0.779	0.770	0.660
Curl	0.923	0.913	0.873	0.905	0.933	0.923	0.890	0.923	0.912	0.907	0.919	0.868	0.902	0.911	0.917	0.902	0.926	0.917	0.974

Sample 1–18 are from the horse coprolite thin section from Petite Rue des Bouchers, phase 4 SU 23; sample 19 is from the dark earth thin section from Poor Clares, SU 415

ND the number of articulated dendritics that were found in each silica skeleton and that formed the wave lobes measured, *NL* number of wave lobes measured in the sample

phytoliths, researchers can have confidence that all the phytoliths in the sample derive not only from the same taxon, but even the same plant, plant part and tissue (Vrydaghs et al. 2015). As discussed above, when at least 30 measurable wave lobes are found in an articulated sample, the five shape measurements of Form factor, Solidity, Convexity, Compactness and Curl can be evaluated with statistical confidence. In theory, if any of those five shape measurements, or combinations of the five measurements, are significantly different between taxa then identification of taxa may be possible even when evaluating a single articulated group, provided it has a sufficient number of dendritics to form 30 measurable wave lobes. As Table 2 indicates, if at least 50 wave lobes are measurable on a single articulated dendritic sample then the variables of Aspect ratio and Roundness could also be evaluated with confidence, while if at least 80 lobes are measurable then the variables of Breadth and Equivalent diameter could likewise be considered and so forth.

After observing the significant variance in wave lobe morphometries within and between accessions of each species we questioned if there was still any potential to use this data to evaluate archaeological samples. In a preliminary effort to explore that potential, we measured the wave lobes of 18 articulated dendritic phytolith samples found in a thin section of a horse coprolite from a site in the historical center of Brussels (Petite Rue des Bouchers, phase 4 SU 23) and one articulated dendritic sample found in a thin section of dark earth from a different site in historical Brussels (Poor Clares, SU 415, for more on the provenance of these samples see Vrydaghs et al. 2015 and the citations therein). The articulated dendritic samples we analyzed each had at least 30 measurable wave lobes that were formed by 8–21 dendritics, which again, allowed us to have statistical confidence in the measurements of Form factor, Solidity, Convexity, Compactness and Curl (cf. Table 2; Fig. 1d is one of the sample images analyzed). Table 3 reports the means for these five morphometries for each of the 19 samples, as well as the number of wave lobes measured on each and the number of articulated dendritics that formed the wave lobes.

As an example of one simple paradigm by which wave lobe reference data might be used in the future to analyze archaeological data, we then compared the means of these five wave lobe morphometries for each of the 19 articulated dendritics from the archaeological thin sections in Table 3 with the range of means observed in each of the known taxa analyzed in this study as summarized in Table 4. While this comparison of archaeological sample means with reference data range of means should not be considered conclusive nor a substitute for the typical statistical analysis of variance between taxa that will be part of our future study, we included it in this report simply to illustrate one way data like that which we have gathered so far might be used in the future.

The results of our simple comparison of the archaeological sample wave lobe morphometry means with the ranges of reference data means are summarized in Table 5. An "X" indicates that the archaeological sample's mean measurement falls within the range of the corresponding reference taxon data. For example, we observe that the articulated dendritic labeled sample "2" in Table 5, which was found in the horse coprolite thin section and had 35 measurable wave lobes (NL = 35) formed by a total of 12 articulated dendritics (ND = 12), has an "X" in the cell for *T. aestivum* compactness. This indicates that the mean compactness measurement for the 35 lobes measured in sample "2" (which was 0.776 as per Table 3) falls within the range of the compactness means observed in our reference data for *T. aestivum* (0.691–0.781 as per Table 4).

The results summarized in Table 5 allow us to make some inferences about the archaeological samples. For

Table 4 Range of means observed in all bract types from all inflorescence locations for all accessions of each species

	aestivum	*dicoccoides*	*Triticum dicoccon*	*durum*	*monococcum*	*Hordeum vulgare*	*Avena sativa*	*Secale cereale*
Size								
Area	21.5–64.1	16.7–35.9	17.5–38.7	12.1–26.3	18.8 – 23.5	5.0–47.1	8.8–32.1	8.3–38.3
Convex area	22.0–67.5	17.3–37.6	18.1–39.7	12.5–26.9	19.8 – 24.9	5.6–48.0	9.0–34.5	8.5–39.7
Perimeter	18.7–33.7	17.0– 24.8	16.9–25.4	14.2–20.7	17.6 – 20.2	10.1–28.1	12.4–24.6	12.1 –25.4
Convex perimeter	17.6–31.5	15.9–23.3	16.0–23.9	13.4–19.5	16.5 – 18.8	9.6–26.5	11.7–22.3	11.5 –23.8
Length	6.5–12.1	6.0–9.8	6.0–9.0	5.1–7.2	6.3 – 7.1	3.9–9.7	4.5–8.3	4.5 –9.1
Fiber length	7.2–13.5	6.9 – 9.3	6.9–10.5	5.8–8.1	7.0 – 8.1	4.5–11.5	5.3–9.6	5.2 –10.2
Breadth	4.7–7.3	3.9 – 5.8	4.0–5.6	3.3–5.1	4.2 – 4.7	1.9–6.5	2.6–5.6	2.5–5.7
Equivalent diameter	5.1–8.7	4.5 – 6.6	4.6–6.8	3.8–5.6	4.7 – 5.3	2.6–7.6	3.3–6.3	3.2–6.9
Inscribed radius	2.0–2.9	1.7 – 2.4	1.6–2.4	1.4–2.2	1.7 – 1.9	0.8–2.8	1.1–2.1	1.0–2.7
Shape								
Form factor	0.670–0.755	0.657–0.771	0.653–0.745	0.684–0.753	0.668 – 0.817	.0644–0.786	0.634–0.721	0.635–0.761
Roundness	0.534–0.641	0.517–0.656	0.531–0.620	0.553–0.640	0.532 – 0.617	0.448–0.631	0.517–0.616	0.504–0.646
Convexity	0.933–0.952	0.937–0.950	0.930–0.948	0.923–0.948	0.935 – 0.949	0.934–0.958	0.911–0.946	0.932–0.953
Solidity	0.950–0.984	0.953–0.985	0.936–0.982	0.944–0.977	0.954 – 0.993	0.950–0.994	0.914–0.978	0.928–0.980
Compactness	0.728–0.799	0.714–0.809	0.724–0.785	0.741–0.799	0.725 – 0.783	0.664–0.796	0.714–0.783	0.706–0.802
Aspect ratio	1.403–1.666	1.379–1.710	1.436–1.805	1.416–1.651	1.490 – 1.710	1.460–2.090	1.422–1.775	1.380–1.844
Elongation	1.585–1.855	1.549–1.963	1.608–2.143	1.619–1.930	1.472 – 1.979	1.683–2.225	1.642–2.056	1.565–2.139
Curl	0.830–0.908	0.857–0.905	0.842–0.894	0.850–0.902	0.864 – 1.045	0.850–0.888	0.850–0.899	0.854–0.891

N 100 wave lobes measured for each mean; all size measurements are in μm or μm^2

example, it appears that samples 1, 3, 5, 7, 8, 9, 11, 12, 13, 15 and 17 have morphometries that fall within the range of most of the taxa in our reference data making it difficult to infer which taxon produced them. In contrast, the morphometries of samples 2, 4, 6, 10, 14, 16 and 18, mostly fall within the range of *T. monococcum* and/or *Hordeum vulgare*. In fact we calculate that 82 % (74 out of 90) of the wave lobe mean measurements for the 18 articulated dendritics from the horse coprolite (samples 1–18 in Tables 3 and 5) fall within the range of those observed in *H. vulgare* while 80 % (72 out of 90) of the mean measurements fall within the range of those observed in *T. monococcum.* The next closet taxa are *Secale cereale* at only 64 % (58 out of 90), *T. dicoccoides* at only 63 % (57 out of 90), and *T. aestivum* at only 62 % (36 out of 90). Mean wave lobe morphometries for *T. dicoccon* and *T. durum* only match the archaeological sample in 44 % of the measurements (40 out of 90), and in only 41 % (37 out of 90) for *Avena sativa.* Thus, if we look at the horse coprolite samples as a whole, and if we were confident that the articulated dendritics in the thin section were likely produced by taxa in our reference data set, then we could reasonably infer that they very likely came from *H. vulgare* and/or *T. monococcum*, and probably not from any of the other taxa included in our reference data. However, because the curl measurements in our horse coprolite samples do not closely match our reference data for *H. vulgare* and the compactness and convexity measurements do not closely resemble those for *T. monococcum,* it may well be that the dendritics in the coprolite are not from a species or accession included in our reference data. Meanwhile, the articulated dendritic from the Poor Clares dark earth thin section (sample 19) showed little resemblance to any taxon in our reference data and most likely did not come from any species or accession in our reference material. Again, these results should be considered illustrative of a way to use and analyze the data rather than as conclusive. To gain more confidence in our analysis using this methodology our next step would be to expand the number of species and accessions in our reference data set, especially including cultivated and wild cereal species and accessions known to be important in the Brussels study region.

Table 5 Comparison of 18 archaeological articulated dendritic wave morphometries with range of mean wave morphometries from all bract types from all inflorescence spike locations for all accessions of each reference species analyzed

	Sample	1	2	3	4	5	6	7	8	9	10	11	12	13	14	15	16	17	18	19
	NL	30	35	30	30	30	40	45	80	40	40	30	30	40	35	30	30	70	30	80
	ND	13	12	13	8	9	11	15	18	16	12	8	9	15	14	12	18	21	13	17
Triticum aestivum	Form Factor	X		X	X	X		X	X	X	X	X	X	X		X		X		X
	Solidity	X		X		X		X	X	X		X				X		X		
	Compactness	X	X			X	X		X	X	X	X		X	X	X	X	X	X	
	Convexity	X	X	X		X		X	X	X	X	X	X	X		X		X		
	Curl			X	X			X			X		X	X			X			
T. dicoccoides	Form Factor	X	X	X	X	X	X	X	X	X	X	X	X	X	X	X	X	X	X	X
	Solidity			X		X		X	X	X		X				X		X		
	Compactness	X	X	X		X	X		X	X	X	X		X	X	X	X	X	X	
	Convexity	X		X		X		X		X	X	X	X	X		X				
	Curl			X	X			X					X	X			X			
T. dicoccon	Form Factor	X		X	X	X		X		X		X	X	X		X				X
	Solidity	X		X				X	X	X		X				X		X		
	Compactness	X	X			X	X		X	X	X	X		X	X	X		X	X	
	Convexity	X		X				X		X		X	X							
	Curl			X				X					X							
T. durum	Form Factor	X		X	X	X		X		X		X	X	X		X				
	Solidity	X		X				X	X	X		X				X		X		
	Compactness	X	X			X	X		X		X	X		X	X	X	X	X	X	
	Convexity	X		X				X		X		X	X							
	Curl			X				X					X	X			X			
T. monococcum	Form Factor	X	X	X	X	X	X	X	X	X	X	X	X	X	X	X	X	X	X	X
	Solidity		X	X	X	X	X	X	X	X	X	X	X	X	X	X	X	X	X	X
	Compactness	X	X			X			X	X	X	X		X	X	X		X	X	
	Convexity	X		X				X		X		X	X	X						
	Curl	X	X	X	X	X	X	X	X	X	X	X	X	X	X	X	X	X	X	X
Hordeum vulgare	Form Factor	X	X	X	X	X	X	X	X	X	X	X	X	X	X	X	X	X	X	X
	Solidity	X	X	X	X	X	X	X	X	X	X	X	X	X	X	X	X	X	X	X
	Compactness	X	X	X	X	X	X	X	X	X	X	X	X	X	X	X	X	X	X	
	Convexity	X	X	X	X	X	X	X	X	X	X	X	X	X	X	X	X	X	X	X
	Curl			X										X						
Avena sativa	Form Factor	X		X	X	X		X		X		X	X							X
	Solidity	X		X				X	X	X		X				X		X		
	Compactness	X	X	X					X	X	X	X		X	X	X		X	X	
	Convexity	X		X				X		X		X	X							
	Curl			X				X					X							
Secale cereale	Form Factor	X	X	X	X	X		X	X	X	X	X	X	X	X	X		X	X	X
	Solidity	X		X		X		X	X	X		X				X		X		
	Compactness	X	X	X		X	X	X	X	X	X	X		X	X	X	X	X	X	
	Convexity	X	X	X		X		X	X	X	X	X	X	X		X	X	X		
	Curl			X				X					X							

Sample 1–18 are from the horse coprolite thin section from Petite Rue des Bouchers, phase 4 SU 23; sample 19 is from the dark earth thin section from Poor Clares, SU 415

NL number of wave lobes measured in the sample, *ND* the number of articulated dendritics that were found in each sample and that formed the wave lobes measured, *X* the mean for the sample falls within the range of means of the reference taxon

Conclusions

This study builds upon previous research aimed at identifying taxa in archaeological samples by their articulated dendritic phytoliths. In this study we have analyzed dendritic wave lobe morphometric variance within five species of wheat and one species each of oats, barley and rye as a precursor to studying variance between the species. We found that within each species there was significant wave lobe morphometric variance between different

accessions of the species and between the different bract types and inflorescences spike locations of the bracts within the accessions of the species. These results suggest that in order to prepare reliable reference data researchers should assure that they sample many accessions for each species, and that all bract types sampled from all inflorescence locations are sampled separately. We further found that shape morphometries are more reliable and require a smaller sample size for statistical confidence than size morphometries when analyzing wave patterns in these taxa. We further observed that smaller sample sizes were adequate for analyzing articulated dendritics compared to those reported to be required for analyzing isolated dendritics. The smaller adequate sample size requirements, and the fact that researchers can have confidence that articulated phytoliths all derive from the same taxon, suggest a promising avenue for eventually identifying cereal taxa in archaeological samples based on the dendritic wave lobe morphometries of a single group of articulated phytoliths. Our analysis of articulated dendritic wave lobes found in thin sections from Brussels illustrates the potential of one method for conducting such research. Whether or not that potential can be realized will need to be further tested and will require greatly expanding our reference data set followed by further tests on archaeological samples.

Acknowledgments We wish to thank the Brussels Capital Region for financing the archaeological research which prompted the present research, the Royal Belgian Institute for Natural Sciences (RBINS) which provided laboratory facilities as well as reference material, and the Research Centre for Agrobiodiversity (Tápiószele, Hungary) for providing the *Triticum monococcum* samples for this study.

References

Albert RM, Shahack-Gross R, Cabanes D, Gilboa A, Lev-Yadun S, Portillo M, Sharon I, Boaretto E, Weiner S (2008) Phytolith-rich layers from the Late Bronze and Iron Ages at Tel Dor (Israel): mode of formation and archaeological significance. J Archaeol Sci 35:57–75

Ball TB, Brotherson JD (1992) The effect of varying environmental conditions on phytolith morphology in two species of grass (*Bouteloua curtipendula* and *Panicum virgatum*). Scan Electron Microsc 6:1,163–1,182

Ball TB, Brotherson JD, Gardner JS (1993) A typologic and morphometric study of phytoliths from einkorn wheat (*Triticum monococcum* L.). Can J Bot 71:1,182–1,192

Ball TB, Gardner JS, Anderson N (1999) Identifying inflorescence phytoliths from selected species of wheat (*Triticum monococcum, T. dicoccon, T. dicoccoides, and T. aestivum*) and barley (*Hordeum vulgare* and *H. spontaneum*). Am J Bot 86:1,615–1,623

Ball TB, Vrydaghs L, Van den Hauwe I, Manwaring J, De Langhe E (2006) Differentiating Banana Phytoliths: Wild and Edible *Musa acuminata* and *Musa balbisiana*. J Archaeol Sci 33:1,228–1,236

Ball TB, Davis A, Evett RR, Ladwig JL, Tromp M, Out WA, Portillo M (2015) Morphometric analysis of phytoliths: recommendations towards standardization from the International Committee for Phytolith Morphometrics. J Archaeol Sci. doi:10.1016/j.jas.2015.03.023

Berlin A, Ball TB, Thompson R, Kittleson D, Herbert SC (2003) Ptolemaic agriculture, "Syrian wheat", and *Triticum aestivum*. J Archaeol Sci 30:115–121

Cabanes D, Weiner S, Shahack-Gros R (2011) Stability of phytoliths in the archaeological record: a dissolution study of modern and fossil phytoliths. J Archaeol Sci 38:2,480–2490

Cotton JM, Hyland EG, Sheldon ND (2014) Multi-proxy evidence for tectonic control on the expansion of C-4 grasses in northwest Argentina. Earth Planet Sci Lett 395:41–50

Devos Y, Nicosia C, Vrydaghs L, Modrie S (2013) Studying urban stratigraphy: Dark Earth and a microstratified sequence on the site of the Court of Hoogstraeten (Brussels, Belgium). Integrating archaeopedology and phytolith analysis. Quat Int 315:147–166

Gillot C (2014) The use of pozzolanic materials in Maya mortars: new evidence from Rio Bec (Campeche, Mexico). J Archaeol Sci 47:1–9

Grund BS, Williams SE, Surovell TA (2014) Viable paleosol microorganisms, paleoclimatic reconstruction, and relative dating in archaeology: a test case from Hell Gap, Wyoming, USA. J Archaeol Sci 46:217–228

Harvey EL, Fuller DQ (2005) Investigating crop processing using phytolith analysis: the example of rice and millets. J Archaeol Sci 32:739–752

Helbaek H (1960) Cereals and weed grasses in Phase A. In: Braidwood RJ, Braidwood LS (eds) Excavation in the plain of Antioch I. University of Chicago Press, Chicago, pp 504–543

Henry AG, Brooks AS, Piperno DR (2014) Plant foods and the dietary ecology of Neanderthals and early modern humans. J Hum Evol 69:44–54

Jenkins E (2009) Phytolith taphonomy: a comparison of dry ashing and acid extraction on the breakdown of conjoined phytoliths formed in *Triticum durum*. J Archaeol Sci 36:2,402

Jones LHP, Handreck KA (1967) Silica in soils plants and animals. Adv Agron 19:107–149

Liu L, Kealhofer L, Chen X, Ji P (2014) A broad-spectrum subsistence economy in Neolithic Inner Mongolia, China: evidence from grinding stones. Holocene 24:726–742

Madella M, Lancelotti C (2012) Taphonomy and phytoliths: a user manual. Quat Int 275:76–83

Madella M, Jones MK, Echlin P, Powers-Jones AH, Moore M (2009) Plant water availability and analytical microscopy of phytoliths: implications for ancient irrigation in arid zones. Quat Int 193:32–40

Out WA, Madella M (2015) Towards improved detection and identification of crop by-products: morphometric analysis of bilobate leaf phytoliths of *Pennisetum glaucum* and *Sorghum bicolor*. Quat Int. doi:10.1016/j.quaint.2015.07.017

Pearsall DM, Piperno DR, Dinan EH, Umlauf M, Zhao Z, Benefer RA (1995) Distinguishing rice (*Oryza sativa* Poaceae) from wild *Oryza* species through phytolith analysis: results of preliminary research. Econ Bot 49:183–196

Pető Á, Gyulai F, Pópity D, Kenéz Á (2013) Macro- and micro-archaeobotanical study of a vessel content from a Late Neolithic structured deposition from southeastern Hungary. J Archaeol Sci 40:58–71

Pető Á, Kenéz Á, Prunner AC, Lisztes-Szabo Z (2015) Activity area analysis of a Roman period semi-subterranean building by means of integrated archaeobotanical and geoarchaeological data. Veget Hist Archaeobot 24:101–124

Phillips C, Lancelotti C (2014) Chimpanzee diet: phytolithic analysis of feces. Am J Primatol 76:757–773

Portillo M, Ball TB, Manwaring J (2006) Morphometric analysis of inflorescence phytoliths produced by *Avena sativa* L. and *Avena strigosa* schreb. Econ Bot 60:121–129

Power RC, Rosen AM, Nadel D (2014) The economic and ritual utilization of plants at the Raqefet Cave Natufian site: the evidence from phytoliths. J Anthropol Archaeol 33:49–65

Qiu Z, Jiang H, Ding J, Yaowu H, Shang X (2014) Pollen and phytolith evidence for rice cultivation and vegetation change during the Mid-Late Holocene at the Jiangli site, Suzhou, East China. PLoS ONE 9:e86,816

Raven JA (1983) The transport and function of silicon in plants. Biol Rev Camb Philos Soc 58:179–207

Rosen AM (1992a) Preliminary identification of silica skeletons from Near Eastern archaeological sites: an anatomical approach. In: Rapp G, Mulholland SC (eds) Phytolith systematics. Plenum Press, New York, pp 129–147

Rosen AM (1992b) Phytoliths as indicators of ancient irrigation farming. In: Anderson-Gerfaud P (ed) Préhistoire l'Agriculture: Nouvelles Approches Expérentales et Ethnographiques. CRNS, Paris, pp 1–7

Sangster AG (1970) Intracellular silica deposition in immature leaves in three species of the Gramineae. Ann Bot 34:245–257

Schultz PHR, Harris S, Clemett SJ, Thomas-Keprta KL, Zarate M (2014) Preserved flora and organics in impact melt breccias. Geol 42:515–518

Shahack-Gross R, Boaretto E, Cabanes D, Katz O, Finkelstein I (2014) Subsistence economy in the Negev Highlands: the Iron Age and the Byzantine/Early Islamic period. Levant 46:98–117

Shillito LM (2011a) Taphonomic observations of archaeological wheat phytoliths from Neolithic Çatalhöyük, Turkey, and the use of conjoined phytolith size as an indicator of water availability. Archaeometry 53:631–641

Shillito LM (2011b) Simultaneous thin section and phytolith observations of finely stratified deposits from Neolithic Çatalhöyük, Turkey: implications for paleoeconomy and Early Holocene paleoenvironment. J Quat Sci 26:576–588

Tromp M, Dudgeon JV (2015) Differentiating dietary and non-dietary microfossils extracted from human dental calculus: the importance of sweet potato to ancient diet on Rapa Nui. J Archaeol Sci 54:54–63

Tubb HJ, Hodson MJ, Hodson GC (1993) The inflorescence papillae of the Triticeae: a new tool for taxonomic and archaeological research. Ann Bot 72:537–545

Twiss PC, Suess E, Smith RM (1969) Morphological classification of grass phytoliths. Soil Sci Soc Am Proc 33:109–115

Umemura M, Takenaka C (2014) Biological cycle of silicon in moso bamboo (*Phyllostachys pubescens*) forests in central Japan. Ecol Res 29:501–510

Veena MP, Achyuthan H, Eastoe C, Farooquic A (2014) A multi-proxy reconstruction of monsoon variability in the late Holocene, South India. Quat Int 325:63–73

Vrydaghs L (2014) Extension Toone, Bruxelles (BR 229). Convention DMS-ARC/CREA-Pat/C-2013-250 entre la Région et le Centre de recherches en archéologie et patrimoine de l'ULB relative aux études paléoenvironnementales. Analyse des modèles de distribution et morphotypologie des phytolithes de l'US 23 du site Extension de Toone (BR 229)

Vrydaghs L, Ball TB, Volkaert H, Van den Houwe I, Manwaring J, De Langhe E (2009) Differentiating the volcaniform phytoliths of bananas: *Musa acuminate*. Ethnobot Res Appl 7:239–246

Vrydaghs L, Ball TB, Devos Y (2015) Beyond redundancy and multiplicity. J Archaeol Sci, Integrating phytolith analysis and micromorphology to study the Brussels Dark Earth. doi:10.1016/j.jas.2015.09.004

Wallis NJ, Cordell AS, Deagan KA, Sullivan MJ (2014) Inter-ethnic social interactions in 16th century La Florida: sourcing pottery using siliceous microfossils. J Archaeol Sci 43:127–140

Zhang J, Lu H, Wu N, Yang X, Diao X (2011) Phytolith analysis for differentiating between foxtail millet (*Setaria italica*) and green foxtail (*Setaria viridis*). PLoS One 6:e19726

Zhao Z, Pearsall DM, Benefer AB, Piperno DR (1998) Distinguishing rice (*Oryza sativa* Poaceae) from wild *Oryza* species through phytolith analysis, II: finalized method. Econ Bot 52:134–135